Quantitative potential measurements of nanoparticles with different surface charges in liquid by open-loop electric potential microscopy

doi: 10.1063/1.3625230

Quantitative potential measurements of nanoparticles with different surface charges in liquid by open-loop electric potential microscopy

Naritaka Kobayashi,[1] Hitoshi Asakawa,[2] and Takeshi Fukuma[1,2,a)]
[1]*Frontier Science Organization, Kanazawa University, Kakuma-machi, Kanazawa 920-1192, Japan*
[2]*Bio-AFM Frontier Research Center, Kanazawa University, Kakuma-machi, Kanazawa 920-1192, Japan*

(Received 25 May 2011; accepted 13 July 2011; published online 25 August 2011)

Local potential distribution plays important roles in physical, chemical and biological processes at a solid/liquid interface. However, the measurement of a local potential distribution in liquid has been a long-standing challenge, which has hindered understanding of the mechanisms for the various interfacial phenomena. Recently, we have developed a method to overcome this problem [Kobayashi *et al*., Rev. Sci. Instrum. **81,** 123705 (2010)], which is referred to as open-loop electric potential microscopy (OL-EPM). Here, we present its first application to quantitative measurements of local potential distribution in liquid. In OL-EPM, an ac bias voltage is applied between a tip and sample and the first and second harmonic cantilever oscillations induced by the electrostatic force are detected and used for the calculation of a potential value. In the equation for the potential calculation, here we introduce a correction factor to cancel out the error caused by the difference in the deflection sensitivity to the first and second harmonic electrostatic forces. With the improved method, we have performed potential measurements of two types of latex beads with different surface charges. The measured potential difference between the different types of latex beads approximately corresponds to their zeta potential difference, which demonstrates the quantitative capability of OL-EPM. © *2011 American Institute of Physics*. [doi:10.1063/1.3625230]

I. INTRODUCTION

Local potential distribution plays important roles in various processes at a solid/liquid interface. For example, adsorption of a particle to a surface and its migration on it are often driven by the local potential distribution. These physical phenomena are closely related to various processes. In biology, local potential distribution is one of the major driving forces to cause an adsorption of proteins or vesicles onto a cellular surface, transportation of ions and molecules along or across a membrane, and conformational changes of proteins. In chemistry, local potential distribution is closely related to the electron transfer involved in electrochemical or catalytic reactions at a solid/liquid interface.

To understand the mechanisms of these processes, it is desirable to directly measure a local potential distribution in liquid. So far, dynamic light scattering (DLS) measurements have often been performed for the determination of a zeta potential value, which is defined as a potential value at the slipping plane.[1,2] However, the method does not allow to measure nanoscale local distribution of the potential. Thus, there have been strong demands for the method to measure local potential distribution at solid/liquid interfaces.

Kelvin probe force microscopy (KFM) (Ref. 3) is a powerful tool which can visualize local potential distribution in air and vacuum on various surfaces such as semiconductor,[4] organic,[5] and biological materials.[6] KFM is usually combined with dynamic mode atomic force microscopy (AFM) (Ref. 7), namely, amplitude modulation AFM (AM-AFM) (Ref. 8) or frequency modulation AFM (FM-AFM) (Ref. 9). However, KFM cannot be operated in liquid. In KFM, the application of ac and dc bias voltages between a tip and a sample induces electrochemical reactions and redistribution of ions and water molecules. These phenomena give rise to uncontrollable spurious forces,[10,11] which not only disturb the stable operation of KFM but also influences structures and properties of a sample.

In our previous study,[12] we developed a method to overcome these difficulties. In this method, only an ac bias voltage with a relatively high modulation frequency $[f_m(\equiv \omega_m/2\pi)]$ is applied between a tip and a sample. The spurious force is greatly suppressed by increasing f_m due to slow time response of electrochemical reactions and redistribution of ions and water molecules. Local potential is calculated from the first and second harmonic oscillation amplitudes (A_1 and A_2, respectively) of a cantilever induced by the application of an ac bias voltage. In contrast to KFM, the method is free from the bias feedback control. Thus, we refer to this method as open-loop electric potential microscopy (OL-EPM). The idea of using two frequency components in dynamic-mode AFM is similar to that of bimodal AFM.[13,14] While bimodal AFM uses the first and second flexural modes of a cantilever, the first and second harmonic frequencies used in OL-EPM are generally lower than the fundamental resonance of the cantilever.

In the previous study, we demonstrated the measurement of nanoscale potential distribution of a dodecylamine thin film on highly oriented pyrolytic graphite (HOPG) in 1 mM NaCl solution by OL-EPM. However, quantitative

a)Electronic mail: fukuma@staff.kanazawa-u.ac.jp.

performance of OL-EPM has not been confirmed due to following reasons. First, the error caused by the frequency dependence of the force sensitivity, which is given by a transfer function $[G(\omega)]$ of a cantilever, was not taken into account. In OL-EPM, a potential value is calculated from the ratio of A_1 to A_2. Thus, the difference between $G(\omega_m)$ and $G(2\omega_m)$ leads to an error in the calculation of a potential value. Second, neither the surface potential nor the zeta potential of the dodecylamine thin film on HOPG in 1 mM NaCl solution was unknown. Therefore, it was difficult to quantitatively evaluate the validity of the potential values measured by OL-EPM.

In this study, to overcome the first problem, we introduce a correction factor (χ) in the calculation of a potential value in OL-EPM. The correction factor is used for compensating the error caused by the difference between $G(\omega_m)$ and $G(2\omega_m)$. We also present a way to determine appropriate values for χ and f_m based on A_1 and A_2 versus f_m curves. To overcome the second problem, we use two types of nanoparticles with different surface charges in the potential measurements by OL-EPM. The zeta potential value of such nanoparticles can be readily measured by DLS measurement. Thus, we evaluate the quantitative performance of OL-EPM by comparing the results obtained by OL-EPM and those obtained by DLS measurement.

II. BASIC PRINCIPLE

In OL-EPM, only an ac bias voltage $[V_{ac}\cos(\omega_m t)]$ with a relatively high modulation frequency is applied between a tip and a sample. A tip-sample electrostatic interaction force (F_{es}) induced by the application of an ac bias voltage is given by

$$F_{es}=\frac{1}{2}\frac{\partial C_{ts}}{\partial z}\left[V_s^2+\frac{1}{2}V_{ac}^2-2V_sV_{ac}\cos(\omega_m t)+\frac{1}{2}V_{ac}^2\cos(2\omega_m t)\right], \tag{1}$$

where C_{ts} and z are tip-sample capacitance and Z position of a tip, respectively. F_{es} contains dc, ω_m, and $2\omega_m$ components (F_{es0}, F_{es1}, and F_{es2}, respectively). In our previous study,[12] we demonstrated that the spurious force (F_{sp}) is sufficiently suppressed at f_m higher than 30 kHz in 1 mM NaCl solution, and hence F_{es1} and F_{es2} are proportional to V_{ac} and V_{ac}^2, respectively.

From Eq. (1), A_1 and A_2 are given by

$$A_1 = G(\omega_m)\left|\frac{\partial C_{ts}}{\partial z}V_s\right|V_{ac}, \tag{2}$$

$$A_2 = G(2\omega_m)\left|\frac{\partial C_{ts}}{\partial z}\right|\frac{V_{ac}^2}{4}. \tag{3}$$

$G(\omega)$ is given by

$$G(\omega)=\frac{1}{k}\frac{1}{\sqrt{[1-(\omega/\omega_0)^2]+[\omega/(Q\omega_0)]^2}}, \tag{4}$$

where k is the spring constant of a cantilever. Equations (2) and (3) indicate that $|V_s|$ can be obtained from the ratio of A_1 to A_2. Thus, $|V_s|$ is given by

$$|V_s| = \frac{G(2\omega_m)}{G(\omega_m)}\frac{A_1}{A_2}\frac{V_{ac}}{4}. \tag{5}$$

The polarity of V_s can be determined by $\cos\phi_1$, where ϕ_1 is the phase difference between the cantilever oscillation at f_m and the ac bias voltage. ϕ_1 ideally takes either 0° or 180° depending on the polarity of V_s. However, in practice, it often shows slight deviation from one of these values owing to the phase delay or noise caused by a cantilever deflection sensor, an ac bias circuit, and/or dielectric material between a tip and a sample. Therefore, $\cos\phi_1$ is used only for the determination of the polarity of V_s as described by

$$\begin{aligned} V_s &= \mathrm{sgn}(\cos\phi_1)\frac{G(2\omega_m)}{G(\omega_m)}\frac{A_1}{A_2}\frac{V_{ac}}{4} \\ &= \mathrm{sgn}(X_1)\frac{G(2\omega_m)}{G(\omega_m)}\frac{A_1}{A_2}\frac{V_{ac}}{4}, \end{aligned} \tag{6}$$

where X_1 is defined by $X_1 \equiv A_1\cos\phi_1$. Here, we define a correction factor χ by the following equation.

$$\chi \equiv \frac{G(2\omega_m)}{G(\omega_m)}. \tag{7}$$

From, Eqs. (5) and (6), V_s is given by

$$V_s = \mathrm{sgn}(X_1)\frac{A_1}{A_2}\frac{V_{ac}}{4}\chi. \tag{8}$$

In our previous study,[12] we assumed that f_m was sufficiently lower than the resonance frequency (f_0) of a cantilever and hence $G(\omega_m) = G(2\omega_m) = 1/k$. This corresponds to the situation where $\chi = 1$ is assumed in Eq. (8). However, this assumption is not necessarily true and χ often shows deviation from 1 as confirmed in the following experiment. Thus, potential values calculated from $\chi = 1$ have contained some error caused by the difference between $G(\omega_m)$ and $G(2\omega_m)$. In this study, we have taken the correction factor χ into account to cancel out this error and have improved the accuracy in the calculation of the potential by OL-EPM.

III. EXPERIMENTAL DETAILS

Figure 1 shows the experimental setup for OL-EPM used in this experiment. OL-EPM was developed by modifying a home-built liquid-environment dynamic mode AFM

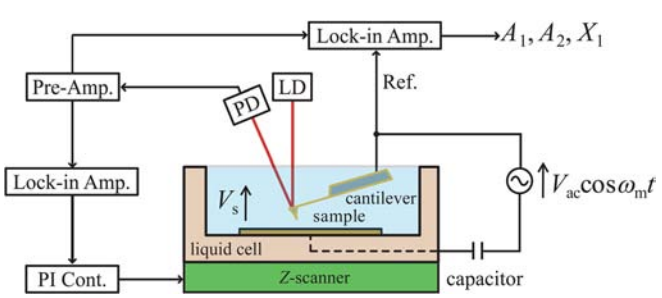

FIG. 1. (Color online) Experimental setup of OL-EPM in liquid. A capacitor is inserted into the bias circuit to prevent an accidental application of a dc bias voltage. A cantilever was excited by piezoactuator, which is not shown here for clarity.

with a low noise cantilever deflection sensor.[15–17] In principle, OL-EPM can be combined with any types of dynamic-mode AFM (Ref. 7) such as AM-AFM, FM-AFM, and phase modulation AFM (PM-AFM). In this study, we combined it with AM-AFM. In AM-AFM, a cantilever is oscillated with fixed excitation amplitude and frequency near the cantilever resonance. The tip-sample distance is controlled such that oscillation amplitude (A) of a cantilever is kept constant. The free oscillation amplitudes (A_0) and amplitude setpoints (A_{sp}) used for the measurements are given in the corresponding figure captions. The oscillation amplitude A was detected with a lock-in amplifier (OC4: SPECS) and the tip-sample distance was regulated with a commercially available AFM controller (RC4: SPECS). A Si cantilever (NCH: Nanoworld) with f_0 of approximately 130 kHz in liquid was used. The cantilever was coated with an Au thin film on the front and back sides (thickness: 50 nm). A digital lock-in amplifier (HF2LI: Zurich Instruments) was used for producing an ac bias voltage and the measurements of A_1, A_2, and X_1.

We used latex beads with surfaces terminated by amino (01-01-251: Micromod) and carboxyl groups (01-02-25 and 01-02-50: Micromod). They are positively and negatively charged in neutral solution, respectively. First, latex beads with amino and carboxyl groups were diluted with pure water to 100 μg/ml and 10 μg/ml, respectively. Then, these solutions are sonicated to prevent aggregation of latex beads for 30 min. After that, one of the diluted solutions was dropped onto a cleaved HOPG surface (ZYA: NT-MDT) and the sample was left for 5 min. The remaining water on the HOPG surface was blown by N_2 gas. The procedure was repeated with the other diluted solution to deposit the two types of latex beads on the same HOPG surface. Finally, the sample was immersed in 1 mM NaCl solution and imaged by OL-EPM.

IV. RESULTS AND DISCUSSION

A. Determination of χ and f_m

In OL-EPM in liquid, f_m should be set at a relatively high frequency but sufficiently lower than f_0. To determine a suitable f_m value, we measured f_m dependences of A_1 and A_2 at $V_{ac} = 1$ V on a cleaved HOPG surface in 1 mM NaCl solution (Fig. 2). At the low f_m range, A_1 and A_2 increase with decreasing f_m due to spurious forces induced by the electrochemical reactions and redistribution of ions and water molecules. The A_1 and A_2 curves also show peaks at $f_m = 130$ kHz and 65 kHz, respectively, owing to the influence from $G(\omega_m)$ and $G(2\omega_m)$.

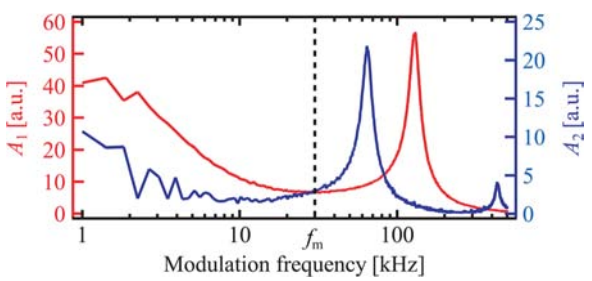

FIG. 2. (Color online) Modulation frequency dependences of A_1 and A_2 measured on an HOPG surface in 1 mM NaCl solution ($f_0 = 130.1$ kHz, $Q = 6.9$). V_{ac} was set at 1 V. The tip-sample distance is set at 100 nm.

In the A_1 and A_2 curves, the spurious force is sufficiently suppressed at the frequency range of $f_m \geq 30$ kHz and $f_m \geq 15$ kHz, respectively. At $f_m = 30$ kHz, $G(\omega_m)$ is almost equal to $1.0/k$ [$G(\omega_m) = 1.06/k$]. Thus, A_1 response is almost free from the influence from $G(\omega_m)$ at this frequency. However, the influence from $G(2\omega_m)$ at $2f_m = 60$ kHz is significantly larger than $1.0/k$ [$G(2\omega_m) = 1.26/k$], and hence not negligible. Therefore, the influence from $G(\omega_m)/G(2\omega_m)$ should be canceled out by the correction factor χ. In this experiment, the value for χ was estimated to be 1.2 by Eqs. (4) and (7). f_0 and Q were determined by fitting a thermal spectrum of the cantilever. We estimated χ in the same way for several cantilevers of the same type and found out that it takes almost the same value under the same experimental conditions. Based on these results, we used $f_m = 30$ kHz and $\chi = 1.2$ in the following experiments for accurate and reproducible measurements.

B. Potential measurements of latex beads with different charges and sizes

We performed potential measurements of latex beads on a cleaved HOPG surface in 1 mM NaCl solution (Fig. 3). The latex beads include the ones with surfaces terminated by amino and carboxyl groups (A-LB and C-LB, respectively). They are positively and negatively charged in neutral solution, respectively. A-LBs used in this experiment have a smaller nominal diameter (25 nm) than that of C-LBs (50 nm). Thus, we are able to differentiate them from size.

In the topographic image [Fig. 3(a)], latex beads with two different sizes are imaged as shown in the height profile [Fig. 3(e)] measured along Line A-B in Fig. 3(a). The height histogram [Fig. 3(g)] of latex beads imaged in Fig. 3(a) shows two peaks. This indicates that latex beads with two different sizes are deposited on the HOPG surface. The average heights of the smaller and the larger latex beads are 26 nm and 68 nm, respectively. These values approximately agree with nominal diameters of A-LB (25 nm) and C-LB (50 nm), respectively. Therefore, we concluded that the smaller and the larger latex beads should correspond to A-LB and C-LB, respectively.

The potential image [Fig. 3(b)] was calculated from the A_1 and A_2 images [Figs. 3(c) and 3(d)] and Eq. (8). X_1 was also recorded for determining the polarity of V_s (not shown here). The potential profile [Fig. 3(f)] measured along Line C-D in Fig. 3(b) shows the existence of latex beads with two different potential values. A comparison between the potential and the topographic images reveals that the potential values measured on larger beads (C-LBs) are smaller than those measured on smaller beads (A-LBs). The potential histogram [Fig. 3(h)] of the latex beads imaged in Fig. 3(b) shows two peaks. This indicates that these latex beads can be classified into two types with different potential. The average of the potential value measured on the A-LBs (i.e., smaller beads) is 70 mV higher than that measured on the C-LBs (i.e., larger beads). This is consistent with the expectation that a positively charged A-LB exhibits a higher surface potential than a negatively charged C-LB. In fact, zeta potential of the

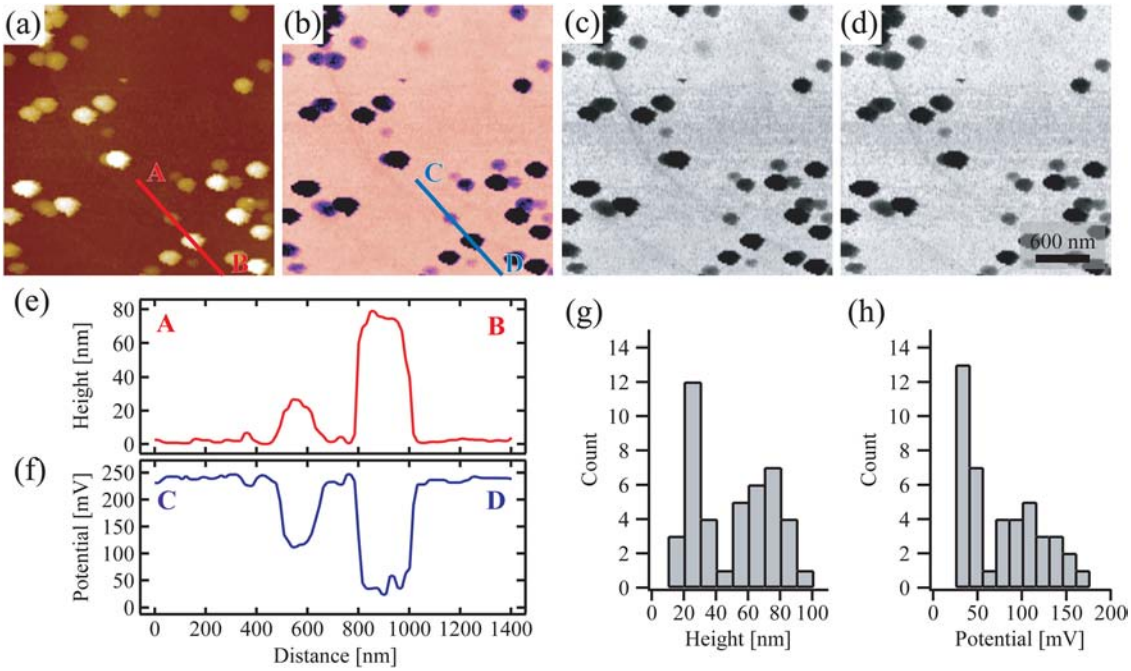

FIG. 3. (Color online) (a) Topographic, (b) potential, (c) A_1, and (d) A_2 images of A-LBs and C-LBs on the HOPG surface in 1 mM NaCl solution (scan size: 3 $\mu m \times 3\ \mu m$, $f_0 = 142.1$ kHz, $Q = 8.2$, $A_0 = 0.67$ nm, $A_{sp} = 0.63$ nm, $f_m = 30$ kHz, $V_{ac} = 1$V, $\chi = 1.2$). (e) Height and (f) potential profiles measured along Line A-B in (a) and Line C-D in (b), respectively. (g) Height and (h) potential histograms of the latex beads imaged in panel (a) and in panel (b), respectively.

A-LBs and C-LBs determined by DLS measurement are 5 mV and −50 mV at pH 7, respectively. The potential difference between the A-LB and C-LB estimated from the OL-EPM image (70 mV) approximately agrees with their zeta potential difference (55 mV).

One of the possible reasons for the 15 mV difference between the results obtained by OL-EPM and DLS measurements is the potential variation in the direction perpendicular to the surface. The zeta potential is defined as the potential at the slipping plane. However, the potential value measured by OL-EPM should reflect the potential averaged over the distance range corresponding to the cantilever oscillation. Therefore, more precise interpretation of the potential values measured by OL-EPM may require measurements of 3D potential distribution, which however is beyond the scope of the present study.

C. Potential measurements of latex beads with the same charge and different sizes

To investigate the influence from the height difference between the latex beads on the potential values measured by OL-EPM, we performed potential measurements of C-LBs (C-LB$_1$ and C-LB$_2$) with two different nominal diameters (C-LB$_1$: 25 nm and C-LB$_2$: 50 nm) (Fig. 4). As they have the same surface termination, they are expected to exhibit the same potential value.

The topographic image in Fig. 4(a) shows latex beads with two different sizes. The height variation of the latex beads is clearly seen in the height profile [Fig. 4(e)] measured along Line A-B in Fig. 4(a). The height histogram [Fig. 4(g)] of the latex beads imaged in Fig. 4(a) shows two peaks. This indicates that latex beads with two different sizes are deposited on the HOPG surface. The average heights of C-LB$_1$ and C-LB$_2$ are 23 nm and 69 nm, respectively. These values approximately agree with their nominal diameters. Therefore, C-LB$_1$ and C-LB$_2$ should correspond to the smaller and the larger beads observed in the topographic image, respectively.

The potential image in Fig. 4(b) was calculated from the A_1 and A_2 images [Figs. 4(c) and 4(d)] and Eq. (8). X_1 was also recorded for determining the polarity of V_s (not shown here). In spite of the height difference between C-LB$_1$ and C-LB$_2$ observed in the topographic image [Fig. 4(a)], all the latex beads show almost the same contrast in the potential image [Fig. 4(b)]. For example, the potential profile [Fig. 4(f)] measured along Line C-D in Fig. 4(b) shows that the potential values measured on the latex beads are almost constant in spite of their height variations [Fig. 4(e)]. The potential histogram [Fig. 4(h)] of the latex beads imaged in Fig. 4(b) shows a single peak. These results demonstrate that the cross talk between the potential measurement by OL-EPM and the height measurement by AM-AFM is negligible. Therefore, the potential variation observed in Fig. 3(b) is unlikely to be caused by such a cross talk but represents the true potential difference between the different types of the latex beads.

V. SUMMARY

In this study, we have introduced a correction factor in the calculation of the potential value in OL-EPM, which improved the quantitative performance of OL-EPM in liquid. With the improved method, we measured the potential difference between the latex beads having positive and negative charges and compared it with their zeta potential difference. The potential difference measured by OL-EPM approximately agrees with their zeta potential difference. We also

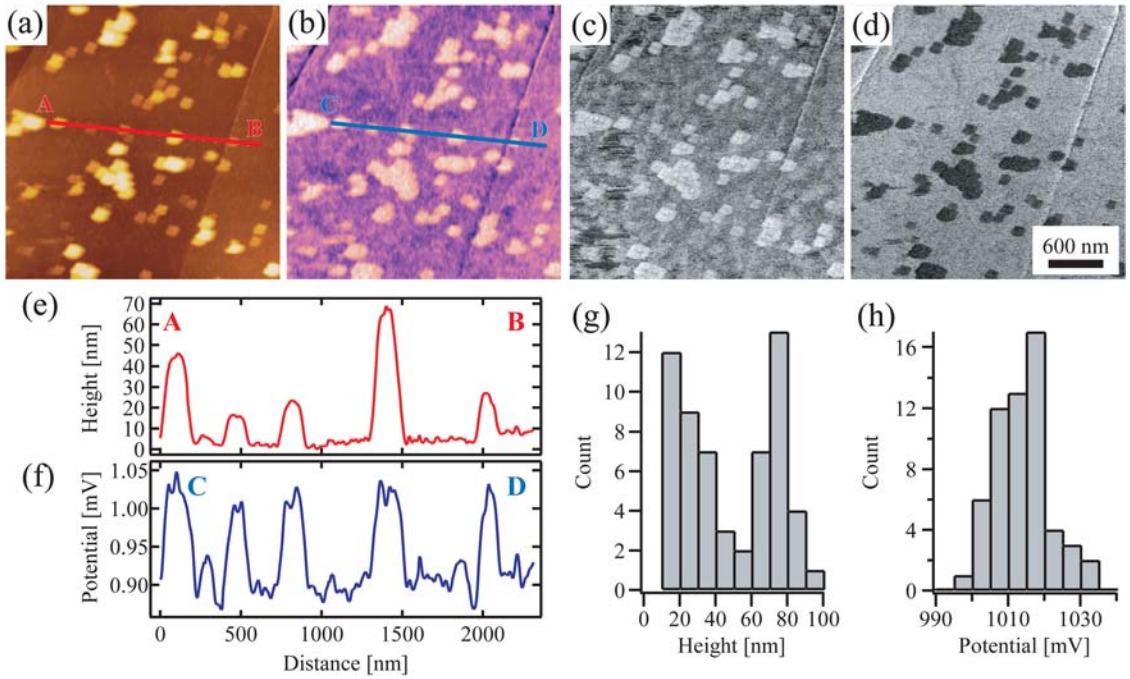

FIG. 4. (Color online) (a) Topographic, (b) potential, (c) A_1, and (d) A_2 images of C-LB$_1$ and C- LB$_2$ in 1 mM NaCl solution (scan size: 3 $\mu m \times 3$ μm, $f_0 = 119.0$ kHz, $Q = 6.7$, $A_0 = 1.4$ nm, $A_{sp} = 1.2$ nm, $f_m = 30$ kHz, $V_{ac} = 1$V, $\chi = 1.2$). (e) Height and (f) potential profiles measured along Line A-B in panel (a) and Line C-D in panel (b), respectively. (g) Height and (h) potential histograms of the latex beads imaged in panel (a) and in panel (b), respectively.

experimentally confirmed that the cross talk between the potential and topographic measurements is negligible in OL-EPM. These results demonstrate that OL-EPM has a capability of quantitative measurement of local potential distribution in liquid.

ACKNOWLEDGMENTS

This work was supported by New Energy and Industrial Technology Development Organization (NEDO) (Grant No. 09A22005a).

[1]G. A. Parks, Chem. Rev. **65**, 177 (1965).
[2]R. H. Yoon, T. Salman, and G. Donnay, J. Colloid Interface Sci. **70**, 483 (1979).
[3]M. Nonnenmacher, M. P. O'Boyle, and H. K. Wickramasinghe, Appl. Phys. Lett. **58**, 2921 (1991).
[4]Y. Rosenwaks, R. Shikler, T. Glatzel, and S. Sadewasser, Phys. Rev. B. **70**, 085320 (2004).
[5]T. Fukuma, K. Umeda, K. Kobayashi, H. Yamada, and K. Matsushige, Jpn. J. Appl. Phys. **41**, 4903 (2002).
[6]C. Leung, H. Kinns, B. W. Hoogenboom, S. Howorka, and P. Mesquida, Nano Lett. **9**, 2769 (2009).
[7]R. Garcia and R. Perez, Surf. Sci. Rep. **47**, 197 (2002).
[8]A. Kikukawa, S. Hosaka, and R. Imura, Rev. Sci. Instrum. **64**, 1463 (1996).
[9]S. Kitamura and M. Iwatsuki, Appl. Phys. Lett. **72**, 3154 (1998).
[10]R. Raiteri and H. J. Butt, J. Phys. Chem. **99**, 15728 (1999).
[11]K. Umeda, N. Oyabu, K. Kobayashi, K. Matsushige, and H. Yamada, Appl. Phys. Express **3**, 065205 (2010).
[12]N. Kobayashi, H. Asakawa, and T. Fukuma, Rev. Sci. Instrum. **81**, 123705 (2010).
[13]C. Dietz, E. T. Herruzo, J. R. Lozano, and R. Garcia, Nanotechnology **22**, 125708 (2011).
[14]R. W. Stark, N. Naujoks, and A. Stemmer, Nanotechnology **18**, 065502 (2007).
[15]T. Fukuma, M. Kimura, K. Kobayashi, K. Matsushige, and H. Yamada, Rev. Sci. Instrum. **76**, 053704 (2005).
[16]T. Fukuma and S. P. Jarvis, Rev. Sci. Instrum. **77**, 043701 (2006).
[17]T. Fukuma, Rev. Sci. Instrum. **80**, 023707 (2009).